

# Characterization of Rubidium-Based Nanoparticles by Green Synthesis and Their Effect on Colorectal Cancer Cells

Dilsad Ozerkan<sup>1</sup> , Ishak Afsin Kariper<sup>2</sup> 

<sup>1</sup>Department of Genetic and Bioengineering, Faculty of Engineering and Architecture, Kastamonu University, Kastamonu, Turkiye

<sup>2</sup>Department of Science Education, Faculty of Education, Erciyes University, Kayseri, Turkiye

ORCID ID: D.O. 0000-0002-0556-3879; I.A.K. 0000-0001-9127-301X

**Cite this article as:** Ozerkan D, Kariper IA. Characterization of rubidium-based nanoparticles by green synthesis and their effect on colorectal cancer cells. *Experimed* 2023; 13(2): 97-102.

## ABSTRACT

**Objective:** Colorectal cancers pose a major threat along with increasing morbidity and mortality to human health worldwide. Therefore, it is crucial to develop effective and safe methods for tumor therapy. In recent years, nanoparticles have emerged as successful candidates for drug delivery into tumor tissues. The particle size of nanoparticles (NPs) is of great importance for passive tumor targeting. Therefore, in this study, we aimed to synthesize and characterize rubidium-based nanoparticles (RbNPs) from the moss *Abietinella abietina* (AA) and determine their anticancer effects on colorectal carcinoma cell line (HCT116).

**Materials and Methods:** A field emission scanning electron microscope (FESEM), dynamic light scattering (DLS), energy dispersive X-ray analysis (EDX), UV/VIS and fourier transform infrared (FTIR) spectrophotometers were used to characterize the RbNPs. To study the cytotoxicity, a sulforhodamine B (SRB) assay was performed in colorectal carcinoma cell cultures.

**Results:** As a result, RbNPs- AA developed with an average particle size of about 70 nm. RbNPs- AA proved to be cytotoxic at lower doses than free AA, as it decreased cell viability at half the amount of free AA (14.25 µg/mL).

**Conclusion:** The availability of RbNPs, particularly for the treatment of colorectal cancer, is evidenced by the fact that all the data collected are highly relevant.

**Keywords:** Colorectal cancer, rubidium nanoparticles, green synthesis

## INTRODUCTION

Besides gastrointestinal cancers, colorectal carcinoma (CRC) is the third most common malignancy and the third leading cause of cancer-related deaths worldwide (1). The most common therapies for CRC include surgery, chemotherapy and radiotherapy for all stages of the disease, and adjuvant and neoadjuvant therapy for advanced stages (2). The fact that symptoms follow a similar course to other bowel diseases and that CRC is not diagnosed until the 3rd and 4th stages, with no response to the treatments used or resistance to treatment, reduces the survival rate for this disease.

Although many alternative methods have been explored, progress is still in its infancy. Tumor-targeted nanostructure systems are therefore heavily involved in cancer research studies (3, 4). In the last 20 years, the environmentally friendly production of chemicals for a sustainable future has been the subject of extensive research worldwide. The choice of an environmentally friendly solvent, an effective reducing agent, and an effective stabilizing agent are the three most important requirements for the production of nanomaterials. However, the biosynthetic method is considered a safe and environmentally friendly green method for the synthesis of nanoparticles for medical purposes. Generally, the chemical methods

**Corresponding Author:** Dilşad Özerkan **E-mail:** dilsadokan@gmail.com

**Submitted:** 19.04.2023 **Revision Requested:** 16.05.2023 **Last Revision Received:** 27.05.2023 **Accepted:** 14.06.2023 **Published Online:** 28.07.2023



Content of this journal is licensed under a Creative Commons Attribution-NonCommercial 4.0 International License.

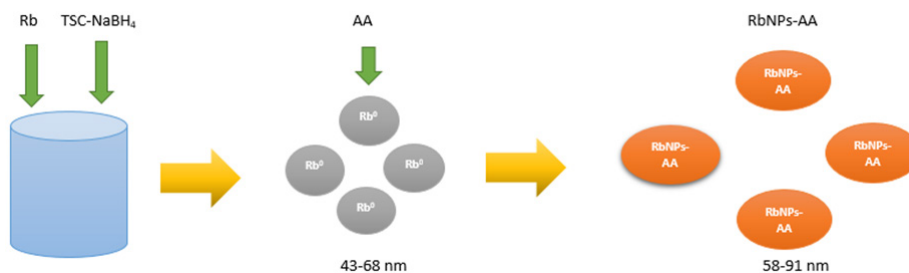


**Diagram 1.** Preparation of RbNPs and RbNPs-AA

used are expensive and involve the use of hazardous and harmful chemicals that pose many risks to the environment (4). Researchers around the world are constantly working on environmentally friendly production techniques that use green nanotechnology to develop highly effective, non-toxic, and environmentally safe products (5). Nanocarriers used in biology and medicine should have low or no toxicity and be easy to integrate and degrade (6). Metallic nanoparticles can easily cross biological barriers and penetrate into human tissues through the pores of the skin. They can bind to proteins and nucleic acids, be absorbed into cell membranes, enter the nucleus and alter the activities of cells, and exhibit greater cellular activity due to their small size and large surface area (7, 8).

The oldest plants, called bryophytes, which can be used in green synthesis, can adapt to a wide range of environmental conditions. They generally have inadequate growth and defense systems. Therefore, liverworts depend on the metabolic processes of secondary metabolites for both survival and environmental protection (9). In addition, some components of the mosses inhibit tumor growth and show an anticarcinogenic effect on various cancer cell lines (10). *Abietinella abietina* (AA) is a moss species from the Thuidiaceae family (11). The discovery of the antileukaemic activity of P-388 in the ethanol extract of *Claopodium crispifolium*, which belongs to the Thuidiaceae family, led to more mosses being collected and studied in 1980 and 1981 (12). Recently, in our work, we investigated different mosses with different extraction solutions, including the cytotoxic effect of AA on the 5-fluorouracil (5-FU) selected CD24+ colon cancer cells. In comparison to many different extracts of AA, the ethanol extract showed the highest cytotoxicity and decreased the Rho123 low cell population in 5-FU resistant HCT116 colon cancer cells (13). Therefore, we wanted to continue this study and analysed the efficacy of ethanol extract of *i* with a nanocarrier at this time. For this reason, rubidium metal-based nanoparticles (RbNPs) were synthesized using AA moss by green synthesis technique and their effects on colon cancer cells (HCT116) were evaluated after their characterization in this study.

## MATERIALS AND METODS

Rubidium dinitrate ( $Rb(NO_3)_2$ ), Sodium borohydride ( $NaBH_4$ ) and trisodium nitrate ( $Na_3C_6H_5O_7$ ) (Sigma Aldrich) were used for RbNPs.  $NaHCO_3$  (Sigma), Dulbecco's modified eagle medium (DMEM; Sigma), dimethyl sulfoxide (DMSO) (Sigma) and fetal bovine serum (FBS) were used for cell culture assays.

### Liverwort Extraction

AA was freeze-dried, and its extracts were obtained. Absolute ethyl alcohol, which has a boiling point of 78.37 °C and a relative polarity of 0.654, was utilized as the dissolvent. A sample-to-solvent ratio of 1:50 was used in the extraction. All of the process was done in the Soxhlet apparatus. After 24 h extraction, the solutions were completely evaporated in a rotary evaporator (Heidolph) at 40°C under a vacuum. For analysis, the powdered dry extracts were diluted with DMSO.

### Preparation of RbNPs and RbNPs-AA

Stock solutions of 0.1 mM  $Rb(NO_3)_2$ ,  $4.3 \times 10^{-3}$  M  $Na_3C_6H_5O_7$ , and  $2 \times 10^{-3}$  M  $NaBH_4$  were prepared. First, 2 mL of  $Rb(NO_3)_2$  was mixed with 24 mL of  $Na_3C_6H_5O_7$  and 24 mL of  $NaBH_4$  for 15 min. at 60 °C. The mixture was then shaken for an additional 15 min. at 90 °C. The obtained RbNPs stock solution was diluted with the extract of 1 mg/mL AA prepared in an aqueous medium (Diagram 1).

### Dynamic Light Scattering (DLS) and Zeta Sizer Analysis

Zetasizer measurements were performed at 22-23°C DLS evaluation with the Zetasizer Nano ZS using a 4 mW He-Ne laser at a wavelength of 633 nm and a detection angle of 173 °C.

### Energy Dispersive X-Ray (EDX)-Field Emission Scanning Electron Microscope (FESEM) analysis

RbNPs and RbNPs-AA samples were trickled onto a glass substrate and covered with Au/Pd at a thickness of 450 nm using a small Polaron sc 7620 sputter coater, then analysed by FESEM and EDX. To image liquid samples for analysis, samples were dropped onto glass substrates, dried, and then placed on the instrument.

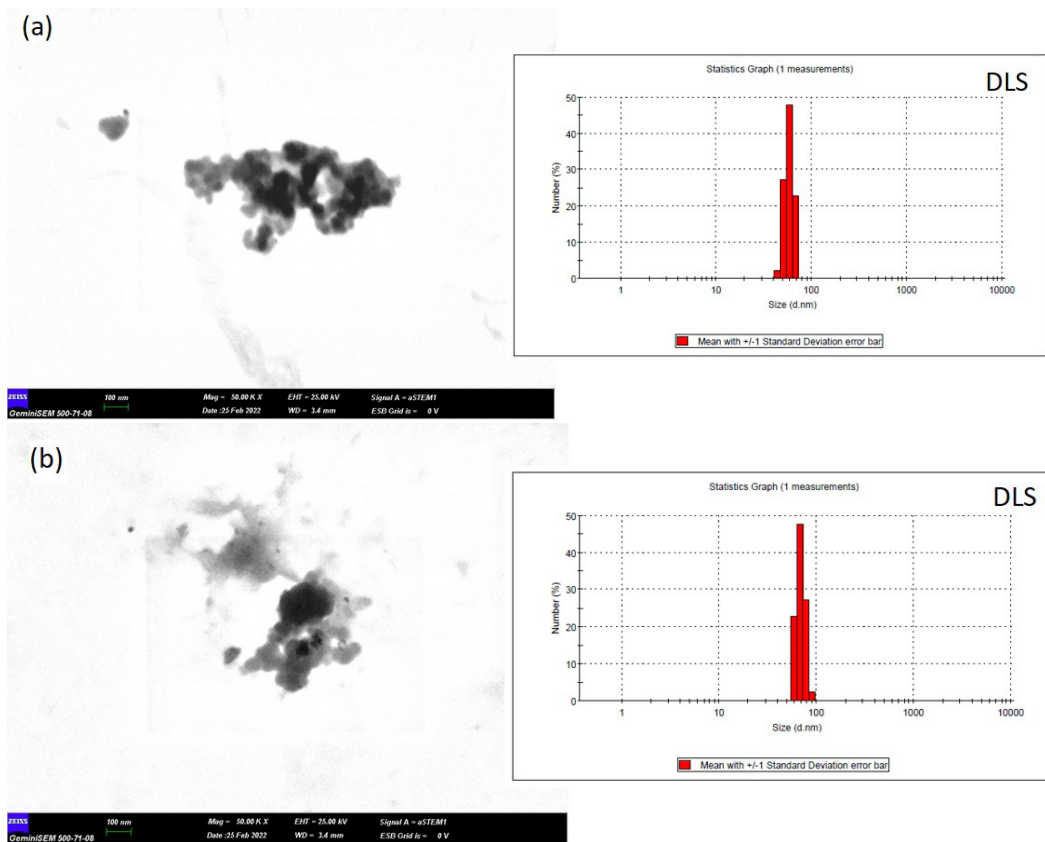


**Figure 1.** FESEM images and DLS particle size distribution of (a) RbNPs and (b) RbNPs-AA.

### Fourier Transform Infrared (FTIR) Analysis of RbNPs and RbNPs-AA

FTIR analyses of the samples were performed using a Perkin Elmer Spectrum (400 FT-IR/FT-FIR Spectrometer Spotlight 400 Imaging System).

### Absorption Measurements

The Hach Lange DR 5000 spectrophotometer was used to evaluate the absorbance of aqueous solutions of plastics. Water was used as a reference for measurements in the wavelength range 200-1100 nm.

### Preparation of Colorectal Carcinoma Cell Line

A total of  $1 \times 10^5$  cells/mL (ATCC® CCL-247™) cells were cultured in DMEM containing 10% FBS and 1% penicilin/streptomycin and incubated at 37 °C in an incubator containing 5% CO<sub>2</sub> for 48 hours.

### Effects of AA and RbNPs-AA on the Cell Viability on HCT116 with Sulforhodamine B (SRB) Assay

SRB is a fluorescent dye that is used to quantify cellular proteins in cultivated cells as well as laser-induced fluorescence. The SRB test determines the volume of all proteins and connects it with the number of cells based on the dye's affinity for amino acids

in proteins in cells (14). For this aim, lyophilized extract stock solutions were prepared in DMSO and then diluted with six different doses of free AA and RbNPs-AA (114, 57, 28.5, 14, 25,

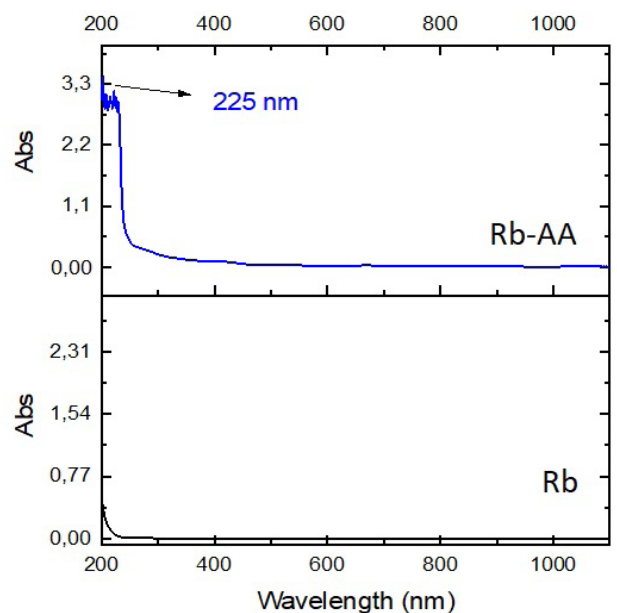


**Figure 2.** UV-VIS measurement results of RbNPs.

7.125, and 3.56 µg/mL) before being administered to HCT116 cells and cultured for 48 hours at 37°C in a 5% CO<sub>2</sub> incubator. After 48 hours, the antiproliferative effect of free AA and RbNPs-AA against colon cancer cells was performed. Dose-response curves were generated to determine the IC<sub>50</sub> of a compound (the concentration that prevents 50% of cells from growing). Using the Graphpad Prism 5 tool, the efficacy of the extracts was compared using this metric.

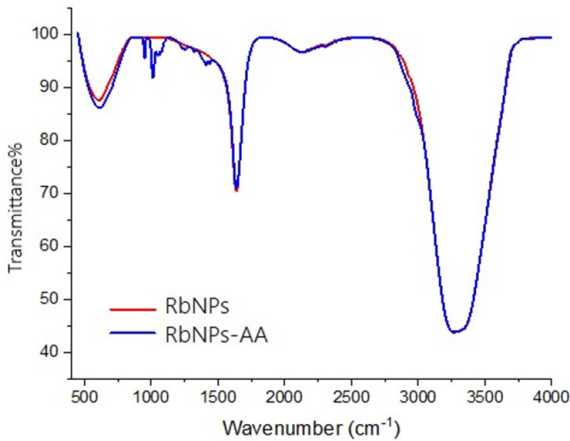


**Figure 3.** The FTIR data of RbNPs, and RbNPs-AA extract.

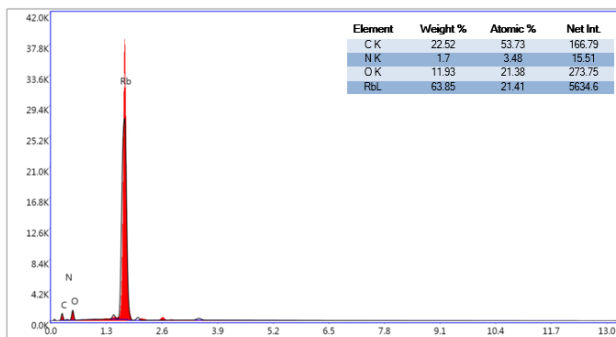


**Figure 4.** EDX analysis of RbNPs-AA.

## RESULTS

In the present work, the size distributions of two RbNPs are compared. The RbNPs produced ranged from 43.82 nm to 68.06 nm, as shown by the DLS data in Figure 1. The approximate particle size is 58 nm on average. The particle diameters of the AA extract linked to RbNPs varied from 58.77 nm to 91.28 nm. FESEM evaluation shows that although the nanoparticles stick together after solvent evaporation, particles between 50 nm and 60 nm are easily visible. In contrast, RbNPs-AA extracts discolored the soil and made it difficult to distinguish particles below 100 nm (Figure 1). This is due to the fact that the amine groups in the extract structure of AA contain dye features.

In the studies of UV-VIS, no pronounced RbNPs absorption peak was detected in the visible spectrum. However, in the composition with the AA extract, strong peaks were detected near the ultra-UV region of 205-225 nm (Figure 2).

In Figure 3, the first peak was shown at 3276 cm<sup>-1</sup> for the -OH band, the second peak was measured at 1645 cm<sup>-1</sup> for the carboxylate group of Na<sub>3</sub>C<sub>6</sub>H<sub>5</sub>O<sub>7</sub>, the band for -CH vibrations at lower wavelengths. Shifts were observed for RbNPs-AA compared to RbNPs. In the RbNPs-AA extract, the -OH vibrational band shifted from 3276 cm<sup>-1</sup> to 3242 cm<sup>-1</sup> due to the amine groups in the structure. Moreover, characteristic vibrational peaks such as -CN stretching, -OH bending, -CH bending, -CO stretching between 1634-1007-934 cm<sup>-1</sup> were measured in the RbNPs-AA group.

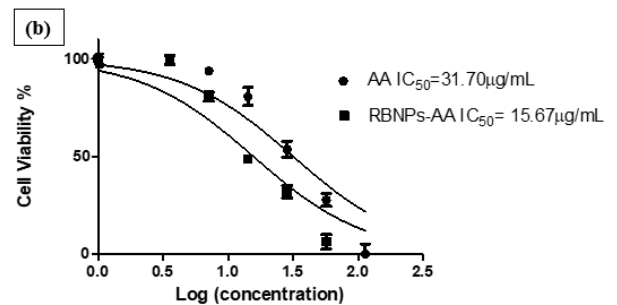
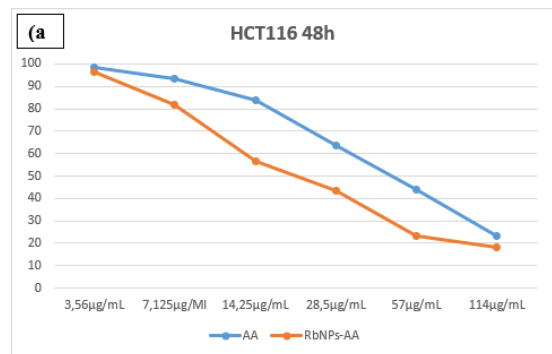


**Figure 5a.** The results of cell viability percentages of RbNPs-AA and free AA. **b.** IC<sub>50</sub> values of RbNPs-AA and free AA.

AA extract had 53.73% carbon, 3.48% nitrogen and 21.38% oxygen, while RbNPs contained 21.41% Rb according to EDX analysis. A very high percentage of the carrier RbNPs was found in the structure (Figure 4).

The effects of nanoparticles on cancer cell viability are determined by cytotoxicity analysis. In this way, the effectiveness of nanoparticles on cells can be better understood. Therefore, the SRB assay was used in this study, which is the preferred cytotoxicity assay. Accordingly, RbNPs-AA inhibited cell viability at half the dose of free AA (14.25 µg/mL) (Figure 5a). When IC<sub>50</sub> values were compared, RbNPs-AA was found to be more cytotoxic (Figure 5b).

## DISCUSSION

To prepare nanoscale pharmaceutical preparations, anticancer drugs have recently been combined with nanoscale matrix materials by covalent chemical bonding, non-covalent chemical interactions (15), encapsulation by hydrophobic interactions, and encapsulation. The water solubility of drugs, distribution in tissues, and *in vivo* pharmacokinetics can be altered using matrix materials, and absorption in cells is also significantly enhanced (16). As a key factor in each stage of nanoparticle packaging, particle size is a crucial characteristic of nanoparticles (17). According to studies (18, 19), small nanoparticles have the advantage of penetrating into tumor tissues, while larger nanoparticles can passively enter the blood and aggregate near tumor blood vessels due to their increased permeability and retention (EPR). The presence of an extracellular matrix (ECM) and anomalous interstitial fluid pressure (IFP) have also been discovered as physiological barriers that contribute to osmotic barriers (20). The force that drives the diffusion of nanomedicines from blood vessels into the tumor is undermined by increased IFP in the tumor, resulting in a lower pressure differential between them (21). A thick barrier that restricts the passage of nanomaterials to the tumor core is formed by the ECM, which includes very active macromolecules that envelop cancer tissue (20). Therefore, it is inconvenient for large nanoparticles to pass through blood vessels and reach the distal end of cancer cells, especially in desmoid tumors that are enclosed by the thick tumor tissue and lack of blood vessels. In another experiment, it was found that 300 nm liposomes enhance the efficacy of surface modification but do not enter the tumor as well as 100 nm liposomes. Clearly, the small particle size of the nanocarrier contributes to a longer half-life of the drug and better tumor penetration. In addition, tumors are prone to collect nanoparticles that have substantial permeability and are below 70 nm in size (22). The average particle size of RbNPs-AA is 70 nm. Thus, the nanoparticle sizes found in this work are quite perfect. In addition, it is possible to determine the size of the particles using XRD patterns and the change in band gap absorption in the UV-VIS spectrum. The strong peaks of RbNPs-AA near the ultra-UV region of 205-225 nm is due to the absorption peaks of the electronic  $\pi^*$  transitions in the AA-extract structure originating from the carboxyl and amine groups (23). FTIR analysis uses infrared beam to scan samples to describe inorganic, organic, and molecular components. A change in chemical structure can be easily detected by changes in the typical pattern of absorption bands. FTIR is useful in defining and identifying unidentified compounds, detecting additions, finding impurities in a substance, and detecting degradation and oxidation (24). While the characteristic vibrational peak of RbNPs was seen at  $596\text{ cm}^{-1}$ , it was simultaneously found that this vibrational signal shifted to  $607\text{ cm}^{-1}$  after AA extraction charge (25). On the other hand, for a thorough chemical evaluation of nanoparticles, EDX has proven to be an effective and quite fast characterization technique (26). In this study significant results were detected by EDX analyzes.

Currently, there are very few studies on the preparation of RbNPs. Rubidium chloride (RbCl)-doped magnesium oxide (MgO) nanoparticles were prepared by Suba et al. (27), using grape juice, and they discovered that these RbNPs have antibacterial properties. A new class of Rb-containing bioactive glass nanoparticles (Rb-BGNs) with particle sizes below 100 nm was prepared in another study, and the results suggested that Rb-BGNs could be effective bioactive fillers for bone regeneration applications (28). According to Khorshid et al. (29), PMF, cesium, and rubidium nanoparticles were found to increase apoptosis in A549 lung cancer cells.

## CONCLUSION

In summary, we have synthesized very small RbNPs with AA extract. The green synthesis approach has remarkable properties suitable for anticancer purposes. This is because the lower dosage of RbNPs-AA, which we used for this study in contrast to the free AA group, proved to be two-fold cytotoxic to colon cancer cells. Bryophytes are plants that do not have to be grown laboriously all over the world, are abundant and contain a lot of bioactive substances. Therefore, they are of great importance for anticancer drug/active substance content. Furthermore, very detailed studies on rubidium nanocarriers have not yet been carried out. So, the efficacy of RbNPs prepared in our work using the green synthesis approach will serve as a model for further studies. Besides, the isolation of biologically active substances from moss extracts could be useful in further investigations of agents providing protection against colorectal cancer.

**Acknowledgement:** The *Abietinella abietina* moss specimens used in the study were obtained from the personal herbarium of Kerem Canlı. We would like to thank him for his invaluable input and support throughout the research process.

**Ethics Committee Approval:** Ethics committee approval is not required for cell culture studies in the article.

**Authors' Contributions:** Conception/Design of Study – D.O., I.A.K.; Data Acquisition – D.O., I.A.K.; Data Analysis/Interpretation – D.O., I.A.K.; Drafting Manuscript – D.O., I.A.K.; Critical Revision of Manuscript – D.O., I.A.K.; Final Approval and Accountability – D.O., I.A.K.

**Conflict of Interest:** Authors declared no conflict of interest.

**Financial Disclosure:** The authors declare that this study has received no financial support.

## REFERENCES

1. Xi Y, Xu P. Global colorectal cancer burden in 2020 and projections to 2040. *Transl Oncol* 2021; 14(10): 101174.
2. Saraiva MR, Rosa I, Claro I. Early-onset colorectal cancer: A review of current knowledge. *World J Gastroenterol* 2023; 29(8): 1289-303.
3. Bonelli J, Velasco-de Andrés M, Isidro N, Bayó C, Chumillas S, Carrillo-Serradell L, et al. Novel tumor-targeted self-nanostructured and compartmentalized water-in-oil-in-water polyurethane-polyurea nanocapsules for cancer theragnosis. *Pharmaceutics* 2022; 15(1): 58.
4. Nath D, Banerjee P. Green nanotechnology - a new hope for medical biology. *Environ Toxicol Pharmacol* 2013; 36(3): 997-1014.

5. Shahverdi AR, Fakhimi A, Shahverdi HR, Minaian S. Synthesis and effect of silver nanoparticles on the antibacterial activity of different antibiotics against *Staphylococcus aureus* and *Escherichia coli*. *Nanomedicine* 2007; 3(2): 168-71.
6. Makarov VV, Love AJ, Sinitynsya OV, Makarova SS, Yaminsky IV, Taliansky ME, et al. "Green" Nanotechnologies: Synthesis of metal nanoparticles using plants. *Acta Naturae* 2014; 6: 35.
7. Ritter SK. EPA Data suggest green success. *Chemical & Engineering News*. 2015; 93: 32–3.
8. Nasrollahzadeh M, Issaabadi Z, Sajadi SM. Green synthesis of a Cu/MgO nanocomposite by *Cassythia filiformis* L. extract and investigation of its catalytic activity in the reduction of methylene blue, congo red and nitro compounds in aqueous media. *RSC Adv* 2018; 8: 3723–35.
9. Clayton WA, Albert NW, Thrimawithana AH, McGhie TK, Deroles SC, Schwinn KE. et al. UVR8-mediated induction of flavonoid biosynthesis for UVB tolerance is conserved between the liverwort *Marchantia polymorpha* and flowering plants. *Plant J* 2018 ; 96: 503–17.
10. Bandyopadhyay A, Dey A. The ethno-medicinal and pharmaceutical attributes of Bryophytes: A review. *Phytomed Plus* 2022; 2: 100255.
11. "*Abietinella abietina* var. *abietina/histicosa*". Royal Botanic Garden Edinburgh. Retrieved 2023-05-18. Available from: URL: <https://www.britishbryologicalsociety.org.uk/wp-content/uploads/2020/12/Abietinella-abietina-var.-abietina-histicosa.pdf>.
12. Spjut RW, Suffness M, Cragg GM, Norris DH. Mosses, hornworts and liverworts screened for antitumor activity. *Economic Botany* 1986; 40: 310-38.
13. Özerkan D, Erol A, Altuner EM, Canlı K, Kuruca DS. Some bryophytes trigger cytotoxicity of stem cell-like population in 5-fluorouracil resistant colon cancer cells. *Nutr Cancer* 2022; 74(3): 1012-22.
14. Orellana EA, Kasinski AL. Sulforhodamine B (SRB) assay in cell culture to investigate cell proliferation. *Bio Protoc* 2016; 6: 21.
15. Andrežalová L, Országhová Z. Covalent and noncovalent interactions of coordination compounds with DNA: An overview. *J Inorg Biochem* 2021; 225: 111624.
16. Sourı M, Soltani M, Moradi Kashkooli F, Shahvandi MK. Engineered strategies to enhance tumor penetration of drug-loaded nanoparticles. *J Control Release* 2022; 3(41): 227–46.
17. Yadav KS, Dalal DC. The heterogeneous multiscale method to study particle size and partitioning effects in drug delivery. *Comput Math Appl* 2021; 92: 134–48.
18. Ikeda-Imafuku M, Wang LLW, Rodrigues D, Shaha S, Zhao Z, Mitragotri S. Strategies to improve the EPR effect: A mechanistic perspective and clinical translation. *J Control Release* 2022; 345: 512–36.
19. Fang J, Islam W, Maeda H. Exploiting the dynamics of the EPR effect and strategies to improve the therapeutic effects of nanomedicines by using EPR effect enhancers. *Adv Drug Deliv Rev* 2020; 157: 142–60.
20. Liu Y, Zhou J, Li Q, Li L, Jia Y, Geng F. et al. Tumor microenvironment remodeling-based penetration strategies to amplify nanodrug accessibility to tumor parenchyma. *Adv Drug Deliv Rev* 2021; 172: 80–103.
21. Zi Y, Yang K, He J, Wu Z, Liu J, Zhang W. Strategies to enhance drug delivery to solid tumors by harnessing the EPR effects and alternative targeting mechanisms. *Adv Drug Deliv Rev* 2022; 114449.
22. Xu J, Song M, Fang Z, Zheng L, Huang X, Liu K. Applications and challenges of ultra-small particle size nanoparticles in tumor therapy. *J Control Release* 2023; 353: 699–712.
23. Jiao Y, Meng F, Zhu G, Ran LZ, Jiang YF, Zhang Q. Synthesis of a novel p-hydroxycinnamic amide with anticancer capability and its interaction with human serum albumin. *Exp Ther Med* 2019; 17: 1321–29.
24. Titus D, James Jebaseelan Samuel E, Roopan SM. Nanoparticle characterization techniques. Shukla AK, Iravani S, editors. *Micro and nano technologies, green synthesis, characterization and applications of nanoparticles*. Elsevier; 2019. p. 303–19.
25. Fissan H, Ristig S, Kaminski H, Asbach C, Epple M. Comparison of different characterization methods for nanoparticle dispersions before and after aerosolization. *Analytical Methods* 2014; 6: 7324–34.
26. Rades S, Hodoroaba VD, Salge T, Wirth T, Lobera MP, Labrador RH. High-resolution imaging with SEM/T-SEM, EDX and SAM as a combined methodical approach for morphological and elemental analyses of single engineered nanoparticles. *RSC Adv* 2014; 4: 49577–87.
27. Suba A, Selvarajan P, Jebaraj Devadasan J. Rubidium chloride doped magnesium oxide nanomaterial by using green synthesis and its characterization. *Chem Phys Lett* 2022; 793: 139463.
28. Ouyang S, Zheng K, Huang Q, Liu Y, Boccaccini AR. Synthesis and characterization of rubidium-containing bioactive glass nanoparticles. *Mater Lett* 2020; 273: 127920.
29. Khorshid FA, Raouf GA, El-Hamidy SM, Al-amri GS, Alotaibi NA. PMF, cesium & rubidium nanoparticles induce apoptosis in A549 cells. *Life Sci J* 2011; 8(3): 534-42.